

# Dynamics of Hippocampal Spatial Representation in Echolocating Bats

Nachum Ulanovsky\* and Cynthia F. Moss

**ABSTRACT:** The “place fields” of hippocampal pyramidal neurons are not static. For example, upon a contextual change in the environment, place fields may “remap” within typical timescales of ~1 min. A few studies have shown more rapid dynamics in hippocampal activity, linked to internal processes, such as switches between spatial reference frames or changes within the theta cycle. However, little is known about rapid hippocampal place field dynamics in response to external, sensory stimuli. Here, we studied this question in big brown bats, echolocating mammals in which we can readily measure rapid changes in sensory dynamics (sonar signals), as well as rapid behavioral switches between distal and proximal exploratory modes. First, we show that place field size was modulated by the availability of sensory information, on a timescale of ~300 ms: Bat hippocampal place fields were smallest immediately after an echolocation call, but place fields “diffused” with the passage of time after the call, when echo information was no longer arriving. Second, we show rapid modulation of hippocampal place fields as the animal switched between two exploratory modes. Third, we compared place fields and spatial view fields of individual neurons and found that place tuning was much more pronounced than spatial view tuning. In addition, dynamic fluctuations in spatial view tuning were stronger than fluctuations in place tuning. Taken together, these results suggest that spatial representation in mammalian hippocampus can be very rapidly modulated by external sensory and behavioral events. © 2009 Wiley-Liss, Inc.

**KEY WORDS:** hippocampus; place cells; spatial map; tetrodes; echolocation; big brown bat (*Eptesicus fuscus*)

## INTRODUCTION

The hippocampus is a brain region crucial for a variety of memory functions (Squire, 1992; Eichenbaum and Cohen, 2001), including spatial memory (O’Keefe and Nadel, 1978; Morris et al., 1982). Rodent hippocampus contains “place cells,” neurons showing spatially selective firing when the animal passes through a certain region of the environment, termed the “place field” (O’Keefe and Nadel, 1978; Wilson and McNaughton, 1993). Place fields are not static, but exhibit changes in their spatial tuning when animals are introduced into a novel environment, or upon certain contextual changes in the environment (Bostock et al., 1991; Wilson and McNaughton, 1993; Mehta et al., 1997; Lee et al., 2004; Leutgeb et al., 2004; Wills et al., 2005). The time constants of these changes are typically on the order of ~1 min, when

measured using a sudden, step-like contextual change. However, these time constants may be largely overestimated, since the assessment of place field dynamics suffers from a “measurement problem,” in that it is necessary to collect at least ~1 min of data in order to properly estimate the place field (Wilson and McNaughton, 1993). In other words, the actual time constants of place field dynamics may be far shorter than 1 min—perhaps as short as seconds or even milliseconds, and this holds important implications for our understanding of the nature and fidelity of hippocampal spatial representation. Indeed, a few studies have shown more rapid changes in hippocampal activity that were linked to *internal* events—either shifts in spatial reference frames (Gothard et al., 1996; Redish et al., 2000; Johnson and Redish, 2007; Jackson and Redish, 2007) or changes within the theta cycle (e.g., Skaggs et al., 1996; Zugaro et al., 2005). However, little is known about rapid place field dynamics in response to external, sensory stimuli. In addition, most of these previous articles (e.g., Gothard et al., 1996; Redish et al., 2000; Johnson and Redish, 2007; Jackson and Redish, 2007) have used population analyzes to demonstrate these rapid dynamics, but did not examine the dynamics of individual neurons; it would be useful to look at individual neurons as well.

Thus, there are several open questions regarding rapid dynamics of hippocampal spatial representation: (i) Do *individual* neurons show rapid dynamics in response to external, *sensory* stimuli? (ii) How fast are the timescales—can we identify very short timescales on the order of hundreds of milliseconds? (iii) Can these dynamics be causally linked to clearly identified sensory events? (iv) What are the implications of modulations in place fields for our understanding of the neural code for space in the hippocampus? To answer these questions reliably requires using thousands of reproducible sensory/behavioral “triggers” that are scattered across a recording session, in order to compute the place fields with fine-grained time windows around those triggers.

Here we studied the dynamics of hippocampal spatial representation on very fine timescales, by utilizing an animal model that naturally provides us with discrete behavioral triggers: the big brown bat, *Eptesicus fuscus*. We have recently shown that the hippocampus of this bat species contains place cells similar to rats (Ulanovsky and Moss, 2007). The dominant mode of sensing in this animal is biological

Department of Psychology and Institute for Systems Research, University of Maryland, College Park, Maryland

Grant sponsor: National Institutes of Health (to C.F.M.); Grant number: MH56366.

\*Correspondence to: Nachum Ulanovsky, Department of Neurobiology, Weizmann Institute of Science, Rehovot 76100, Israel.

E-mail: nachum.ulanovsky@weizmann.ac.il

Accepted for publication 22 September 2009

DOI 10.1002/hipo.20731

Published online 15 December 2009 in Wiley Online Library (wileyonlinelibrary.com).

sonar (echolocation), a high-resolution distal sensing system that relies on the production of discrete sonar calls, in order to create an “acoustic image” of the environment based on the returning echoes (Ulanovsky and Moss, 2008). Hence, the brief sonar calls of the bat could be used as triggers for fine temporal analysis of place-field dynamics. We show here that indeed hippocampal place fields of the big brown bat changed with time constants of a few hundred milliseconds: Place fields were smallest immediately after an echolocation call, when the returning echoes from the environment brought a wealth of sensory information, and then place fields rapidly broadened, or “diffused,” with the passage of time after the call. We also used as behavioral triggers the transition points between two distinct exploratory behaviors in the bat, and showed dynamic changes in place fields and in their directional properties, on a timescale of seconds. Finally, we discuss the functional implications of these rapid time constants, and provide experimental predictions for rodent hippocampal place cells.

## METHODS

### Subjects and Behavioral Training

Experimental procedures were approved by the Institutional Animal Care and Use Committee at the University of Maryland, College Park, and are detailed elsewhere (Ulanovsky and Moss, 2007). The bat species used here—the big brown bat, *Eptesicus fuscus*—was the same as in our previous study (Ulanovsky and Moss, 2007). In brief, two adult big brown bats (weight 18 and 15 g) were trained to crawl in a  $68 \times 73$ -cm rectangular arena, in search of mealworms hung at random locations (“mealworm-chasing” task). The arena was tilted  $70^\circ$  above horizontal, and bats crawled only on the tilted “wall.” Polystyrene balls were hung on the arena walls in an asymmetric arrangement, and served as landmarks.

At the start and end of each recording day, the arena was thoroughly cleaned with alcohol, to remove odors. Each recording day consisted of two 20-min behavioral sessions: “session 1” (lights-off, bat relied solely on echolocation) and “session 2” (dim lights on), interspersed with three sleep sessions. The two behavioral sessions were originally designed for another study (Ulanovsky and Moss, 2007), but we found that big brown bats, in which echolocation is the overwhelmingly dominant sensory modality (Griffin, 1958), produced sonar calls with almost identical intercall intervals in the two sessions (mean intervals: 236 and 237 ms, respectively); therefore, echolocation-related changes in neuronal firing were later averaged across the two sessions (see “Data analysis” below).

### Surgery and Recording

After learning the mealworm-chasing task, the bats were implanted with a four-tetrode microdrive (weight 2.1 g; Neuralynx, Tucson, AZ), which was loaded with tetrodes constructed

from four strands of  $12.7\text{-}\mu\text{m}$  nichrome wire; tetrodes were gold plated to reduce wire impedance to  $0.5\text{--}1.0\text{ M}\Omega$  (at 1 kHz). The microdrive was implanted above the right dorsal hippocampus, 1.8-mm lateral and 2.6-mm anterior to lambda, and tetrodes were slowly lowered towards CA1 pyramidal layer; positioning of tetrodes in the layer was provisionally determined by the presence of high-frequency field oscillations (“ripples”) and associated neuronal firing, and was later verified histologically (Ulanovsky and Moss, 2007). One of the tetrodes was placed in an electrically quiet zone and served as a reference (location of this reference in bat 1: at brain surface, above the hippocampus; in bat 2: white matter, medial to the lateral ventricle). The remaining three tetrodes served as recording probes, although in each bat we obtained high-quality recordings from only one tetrode. During recordings, a unity gain preamplifier (HS-16, Neuralynx) was attached to a connector on the microdrive. The microdrive’s weight was balanced by a small counter weight via a pulley in the ceiling. Signals were amplified ( $2,000\times$ ) and band-pass filtered (600–6,000 Hz, Lynx-8, Neuralynx), and a voltage-threshold was used for collecting 1-ms spike waveforms, sampled at 32 kHz. We also collected continuous recordings of the local field potentials from each of the tetrodes ( $1,000\times$  gain, 1–475 Hz filtering, 2 kHz sampling rate). A video tracker (Neuralynx) recorded the positions of two light-emitting diodes on bat’s head at a 30-Hz rate, and the center-of-mass of the two diodes was used to estimate the bat’s  $x$ - $y$  position; the colors of the two diodes were different (either red/blue or red/green), allowing estimation of the bat’s head direction. Echolocation calls were recorded via a bat detector (D-230, Pettersson Elektronik, Sweden) feeding into the data acquisition system (Neuralynx Cheetah). Data were collected continuously throughout each recording day ( $\sim 2$  h/day).

### Spike Sorting

Spike waveforms were separated based on relative energies on 3 channels of each tetrode, using software that allowed three-dimensional rotations and translations of these data (SpikeSort3D, Neuralynx). Data from all five sessions were spike sorted together. Well-isolated clusters of spikes were manually circled (“cluster-cutting”), and a refractory period ( $<2$  ms) in the interspike-interval histogram was verified. Putative pyramidal cells were identified based on (i) spike waveform, (ii) firing-rate  $<5$  Hz, (iii) interspike interval histograms indicating complex-spike bursts, and (iv) the simultaneous recording of other complex spike cells (see details in Ulanovsky and Moss, 2007). Figure 1 shows an example of spike sorting of data recorded from one tetrode. A total of 154 well-isolated pyramidal neurons were recorded from two bats for this study; these are the same 154 neurons as the ones reported in Ulanovsky and Moss (2007).

### Data Analysis

For analyzing firing-rate maps (place fields) of neurons, we partitioned the arena into  $5 \times 5$ -cm bins, and divided the

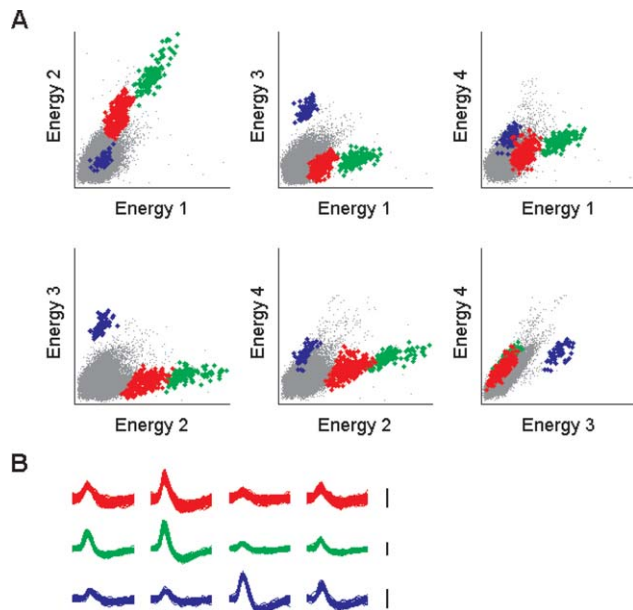


**FIGURE 1.** Spike sorting (cluster cutting) of data recorded from one tetrode, showing all the spikes from the five behavioral sessions of one day. (A) Energy display (“cluster plots”) showing the energy of spikes (dots) on two of the tetrode’s four channels; each of the six panels shows a different combination of two channels. Three single units are seen (three clusters, colored separately). Gray dots, small spikes or noise that crossed the voltage threshold but were not classified as single units. (B) Waveform display: spike waveforms from the three units (rows) on all four tetrode channels (columns), with colors corresponding to the clusters in A; all the waveforms, from all the five sessions, are shown superimposed. Vertical scale bars, 200  $\mu$ V; waveform duration, 1 ms.

number of spikes by the time the animal spent within each bin (excluding bins with  $<1$  sec time spent). For display purposes, firing-rate maps were smoothed with a  $3 \times 3$ -bin triangular window. Maps were computed separately for each behavioral session.

We also computed maps separately for spikes that occurred in different time-windows after the most recent preceding echolocation call (time 0). Four time windows were used: 0–78, 78–185, 185–400, and  $>400$  ms (session 1), or 0–78, 78–210, 210–540, and  $>540$  ms (session 2); these particular windows were chosen to equalize the average number of spikes across the four time windows (Fig. 3E; one-way analysis of variance (ANOVA) of the population spike counts per window, over time windows #1, 2, 3, 4:  $P > 0.9$ ). We analyzed only well-isolated pyramidal neurons which met the following spike-count criterion: In at least one behavioral session, the cell discharged  $>400$  spikes/session and also  $>100$  spikes/session in *each* of the four time windows. All the cells which met this spike count criterion ( $n_{\text{cells}} = 32$ ) also had well-defined place fields. [The number of place cells used in this analysis,  $n_{\text{cells}} = 32$ , is smaller than the 47 place cells reported in Ulanovsky and Moss (2007), since in the previous study the inclusion criterion for

spike numbers was that a neuron had to discharge  $>100$  spikes/session, whereas here we required  $>400$  spikes/session and  $>100$  spikes/session in *each* of the four time windows; hence a smaller number of cells met the inclusion criterion for the current analysis. Also, note that not all cells were recorded in both of the behavioral sessions. We had more cells that met the spike count criterion for behavioral session 2,  $n_{\text{cells}} = 28$ , than in session 1,  $n_{\text{cells}} = 22$ ; the union of these 28 and 22 cells that met our inclusion criteria resulted in our total number of cells,  $n_{\text{cells}} = 32$ .]

To quantify the spatial selectivity of place fields, we used three standard indices (Skaggs et al., 1993, 1996; Markus et al., 1994; Save et al., 2000; Ulanovsky and Moss, 2007): (i) Spatial information (bits/spike) =  $\sum p_i(r_i/r) \log_2(r_i/r)$ , where  $r_i$  = the cell’s firing rate in the  $i$ -th bin of the place field,  $p_i$  = probability of the animal being in the  $i$ -th bin (time spent in  $i$ -th bin/total session time), and  $r$  = overall mean firing rate. (ii) Sparsity =  $\langle r_i \rangle^2 / \langle r_i^2 \rangle = (\sum p_i r_i)^2 / \sum p_i r_i^2$ . (iii) Spatial coherence = correlation between the firing rate map and the firing rate averaged across the eight neighbors of each bin; coherence was computed from nonsmoothed maps, and was Fisher Z-transformed. After computing the above three indices, we then computed a combined “spatial selectivity index” (SSI), separately for each cell ( $n_{\text{cells}} = 32$ ) and each time window ( $n_{\text{windows}} = 4$ ), as follows: First, for each of the three indices (spatial information, sparsity, coherence) we averaged the values in the two behavioral sessions, separately for each time window; in cells for which only one session met the spike count criterion, this session’s data were used. Second, for each index we computed the difference between time window # $j$  and time window #1, divided this by the average of the two time windows, and multiplied  $\times 100$ , yielding normalized indices reflecting the percentage change from time window #1. Third, we computed the SSI for each neuron and each time window, by averaging:

$$\text{SSI} = (\Delta \text{Information}_{\text{norm}} - \Delta \text{Sparsity}_{\text{norm}} + \Delta \text{Coherence}_{\text{norm}}) / 3$$

where a minus sign preceded the sparsity, because an increase in sparsity indicates a decrease in spatial selectivity (Skaggs et al., 1996).

We computed the peristimulus time histogram (PSTH) for the spikes of each neuron by using the bat’s echolocation calls as triggering events (time 0), and calculating the neuron’s firing rate in 1-ms bins (taking only calls flanked by an interval of at least 100 ms before the call onset and 400 ms after, without any intervening calls). To test for auditory spiking responses, we did a two-tailed  $t$ -test on the PSTH of each neuron, comparing the last 100 ms precall vs. the first 300 ms postcall; this and all other statistical tests in this study were considered significant when  $P < 0.05$ .

We also computed the “spatial view field” of each neuron (Rolls, 1999), in a manner analogous to the computation of place fields. Namely, we partitioned the walls of the arena into 56 bins (14 on each wall), and for each bin we divided the number of spikes that were emitted while the animal directed

its head and sonar beam toward that bin on the wall, by the total time the animal spent directing its sonar beam at that bin (excluding bins with <1 sec time spent). Spatial view fields for each neuron were plotted using a color-coded scale, similar to the display of place fields (see e.g., Fig. 4).

Finally, we defined the behavioral state of the animal, as illustrated in Figure 5A: We computed the linear velocity and angular velocity of the bat in an 8-sec sliding window, and for each 33-ms video frame we assigned the bat to a behavioral state that was either “locomotion” or “wall-scanning,” depending on whether the 8-sec data segment centered around that frame showed higher-than-median *linear* velocity (Fig. 5A, red) or higher-than-median *angular* velocity (Fig. 5A, blue), respectively. (We computed the linear velocity and angular velocity also with other time windows, apart of the 8-sec window, and these gave similar results.) Intuitively, these two behavioral states can be thought of as representing the animal exploring the environment by locomoting, similar to the way a rat or a mouse would explore their environment (“locomotion mode”)—or the animal exploring the environment by repetitively moving its head from left to right and using its echolocation system to explore the environment from a distance (“wall-scanning mode”). For the analyses in Figures 5 and 6, the place fields and spatial-view fields were computed separately for each of the two behavioral states, by using only the spikes and the video frames that matched one behavioral state or the other.

## RESULTS

### Rapid Dynamics of Bat Hippocampal Place Fields After Each Echolocation Call

Big brown bats produce brief ultrasonic calls with durations of a few milliseconds, and use returning echoes to orientate in the environment (Griffin, 1958; Schnitzler et al., 2003; Ulanovsky and Moss, 2008). In a restricted experimental setup with dimensions of ~1 m, all echoes return within <6 ms after each call (echoes return from the walls and landmarks of the arena with delays approximately 58  $\mu$ sec/cm distance). However, in crawling big brown bats, the intercall intervals may reach hundreds of milliseconds, or even >1 sec (Ulanovsky and Moss, 2007). Thus, echolocation serves as a temporally discrete, strobe-like system, where each call brings a brief influx of sensory information, followed by a long pause, during which no echo information arrives. This feature allowed us to use the timing of bat calls as alignment-points (time 0) around which we averaged the activity of hippocampal place-cells, permitting us to measure place field dynamics with temporal resolution that is difficult to reach otherwise.

As described in the Methods, we trained bats to search for mealworms in a rectangular arena, and recorded head position and echolocation calls as the animals performed two behavioral sessions every day. Tetrodes were used to record the activity of well-isolated pyramidal neurons from hippocampal area CA1

(Fig. 1; Ulanovsky and Moss, 2007). To assess the neural dynamics following an echolocation call, we measured the relative timing between each spike and its immediately-preceding call (Fig. 2A), and parsed spikes into four groups, based on the time window in which the spike occurred. Place-fields were then computed separately for each of the four time-windows (Fig. 2B). These time windows were selected to equalize the average number of spikes/time-window (one-way ANOVA of the population spike counts per window, over time-windows #1, 2, 3, 4:  $P > 0.9$ ). We included in our analyses all the place-cells that discharged >100 spikes/session in each of the four time-windows ( $n_{\text{cells}} = 32$ ).

Hippocampal place cell activity tended to change with the passage of time after the sonar call, as shown in the examples in Figure 2B: The place-field of the first neuron (cell 1) broadened over time, whereas the second neuron (cell 2) showed an increase in out-of-field background firing (cyan color) - both changes implying a reduced spatial-selectivity. To quantify these dynamics, we computed three commonly-used indices of spatial selectivity: Two indices that are positively correlated with spatial-selectivity (*spatial information* and *coherence*) and one index that is negatively correlated with spatial selectivity (*sparsity*; see Methods). For both of the cells shown in Figure 2, the spatial information and coherence decreased and the sparsity increased over time, indicating rapid reduction in spatial-selectivity (Fig. 2C).

Next we examined the population average changes in spatial-information, sparsity and coherence across the four time windows (Fig. 3A). Because the echolocation behavior was virtually identical in the two sessions (see Methods), we combined for each neuron the data from both sessions (Fig. 3A, Insets). These plots indicated the same result, namely a statistically significant decrease in information and coherence and an increase in sparsity over time (one-sided *t*-tests of time windows #2, 3, 4, pooled together, vs. time-window #1: *information* decreased:  $t = 2.50$ ,  $df = 95$ ,  $P < 0.01$ ; *sparsity* increased:  $t = 3.25$ ,  $df = 95$ ,  $P < 0.001$ ; *coherence* decreased:  $t = 2.89$ ,  $df = 95$ ,  $P < 0.003$ ). In order to use a single index of spatial selectivity, we took the combined data from the two sessions, converted them to percentage change, and then averaged the percentage change in spatial information, sparsity and coherence—resulting in a “spatial selectivity index” (SSI), reflecting the changes in hippocampal neurons’ spatial selectivity in time-windows #2, 3, 4 compared with time window #1 (Fig. 3B; see Methods). The SSI exhibited a nearly linear decrease over time (Fig. 3B, right).

The decrease in spatial selectivity between time window #1 and time window #4—within a time span of ~1 sec—was not large in size, but was statistically significant: On average, the SSI decreased by 16% ( $n_{\text{cells}} = 32$ : one-sided *t*-test,  $P < 0.001$ ). A decrease in spatial selectivity was seen in most individual cells (SSI < 0: 23/32 cells, 72%) (Figs. 3B,C). Furthermore, in almost one third of the cells the spatial-selectivity decreased by more than 30% (Fig. 3C, SSI < -30: 10/32 cells, 31%), and in some cells the spatial selectivity decreased by more than 50% (4/32 cells, 13%). Some extreme cases (e.g.,

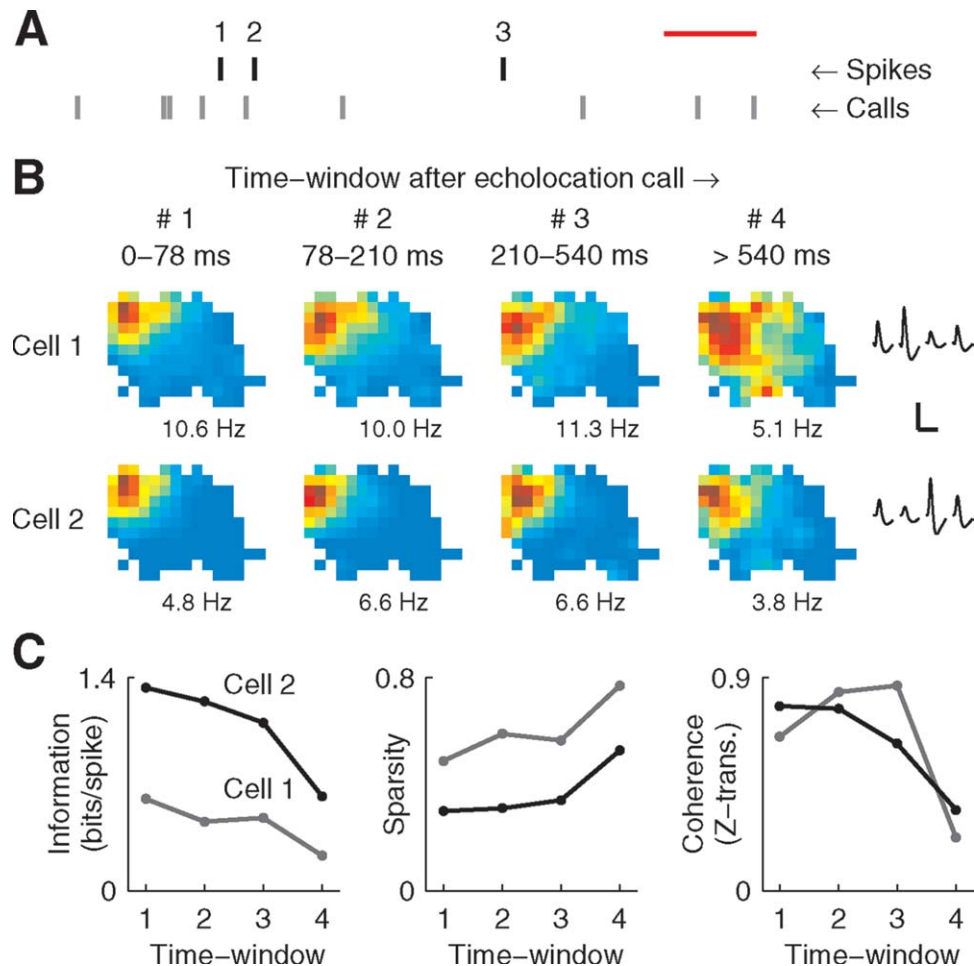


**FIGURE 2.** Rapid dynamics of bat hippocampal place fields following an echolocation call: examples. (A) Sequence of echolocation calls of a big brown bat (gray ticks) and three spikes recorded from a single pyramidal cell (black ticks). Red scale bar, 300 ms. Time differences between spikes no. 1, 2, 3 and their preceding echolocation calls: 58, 29, 521 ms, respectively. Here we asked whether spikes occurring late after an echolocation call (e.g., spike no. 3) conveyed less spatial information than spikes occurring early after a call (e.g., spikes no. 1 and 2). (B) Examples of two neurons (rows) in which the place-field changed with the pas-

sage of time after the echolocation call (columns): The place-field of the first neuron (cell 1) broadened over time, whereas the second neuron (cell 2) showed mostly an increase in out-of-field firing. Linear color scale: light blue, zero firing-rate; red, peak firing-rate (indicated). Waveforms on the right: average spike-shapes of each cell on the tetrode's four wires: scale bars, 1 ms and 100  $\mu$ V. (C) Plots of three indices that quantify the spatial-selectivity of place-fields: spatial information, sparsity, coherence (Z-transformed). Cell 1, gray; cell 2, black.

Fig. 2B, cell 1) showed a progressive increase of place field size by a factor of 2, or more.

Linear regression between the SSI and the time-after-call yielded the following regression-equation:

$$\text{SSI}(\text{predicted}) = 1.7 - 20.0 \times \text{times-after-call}$$

where SSI was measured in percent and time-after-call in seconds. This regression was statistically significant ( $R^2 = 0.21$ ,  $P < 10^{-7}$ ; based on  $n = 128$  data points = 32 cells  $\times$  4 time-windows; 95% confidence-intervals on the time-after-call coefficient:  $-27.0$  to  $-13.0$ ). Importantly, multiple linear regression on three variables—time-after-call, call rate, and locomotion velocity—showed that only the time-after-call contributed significantly to the regression, whereas the bat's

call-rate and its crawling velocity did not contribute to the regression (data not shown); hence, the changes in place fields were the result of time-after-call per se.

In addition to changes in tuning, *peak* firing rates of place fields also changed, becoming slightly lower after  $\sim 1$  sec (Fig. 3D; one-way ANOVA,  $P < 0.03$ ; post hoc *t*-test (corrected for multiple comparisons) for time window #4:  $P < 0.05$ )—although the *average* spike-counts in all the four time windows did not change significantly (Fig. 3E; one-way ANOVA,  $P > 0.9$ ). This suggests that the spatial tuning for at least some place cells did not only broaden, but was also somewhat quenched. Hence, these place-fields could be described as 'diffusing' over time.

Taken together, the analyses reported above reveal the following: (i) within the first 1-sec after a call, place cells lost on

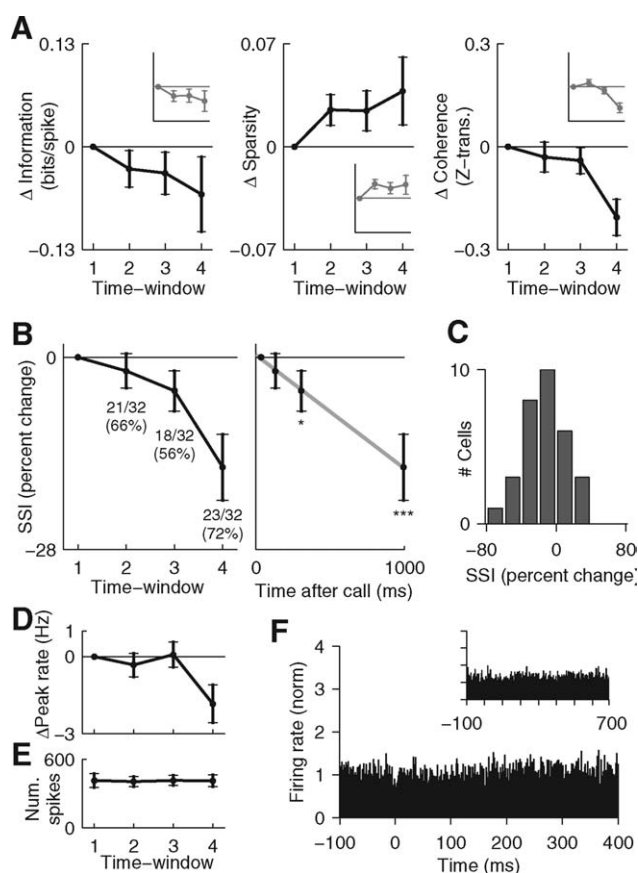


**FIGURE 3.** Rapid dynamics of bat hippocampal place fields following an echolocation call: population analysis. (A) Left, population average changes in spatial-information compared with time-window #1 ( $\Delta$ information); middle, change in sparsity ( $\Delta$ sparsity); right, change in coherence ( $\Delta$ coherence). Errorbars, mean  $\pm$  S.E.M., here and elsewhere. Main plots, behavioral session 2 ( $n_{\text{cells}} = 28$ ). Insets, combined sessions 1 and 2 ( $n_{\text{cells}} = 32$ ). (B) Left, spatial selectivity index (SSI) vs. #time-window ( $n_{\text{cells}} = 32$ , see Methods); shown also are the numbers and proportions of cells with SSI  $< 0$  in each time-window. Right, SSI vs. the median time-after-call of spikes in each window; gray line, best linear fit, demonstrating that SSI decreased over time in a nearly-linear manner. Stars, one-sided  $t$ -tests: \* $P < 0.05$ ; \*\*\* $P < 0.001$ . Note that all the echoes from the environment returned to the bat well within time-window #1—so the changes in hippocampal spatial selectivity occurred when no acoustic information was arriving anymore. (C) Distribution of SSI values in time-window #4 ( $n_{\text{cells}} = 32$ ). (D) Changes in the peak firing-rate of place fields; data from session 2. (E) Numbers of spikes per time-window, showing that the four time-windows contained on average the same number of spikes (these time-windows were chosen to equalize the average spike-numbers). Data from session 2; the plot for session 1 was very similar. (F) Peri-stimulus time histogram (PSTH), showing that place-cells did not exhibit auditory spiking responses to echolocation-calls. Main plot: Population average PSTH, computed for the same neurons as in B ( $n_{\text{cells}} = 32$ ); the PSTH of each neuron was normalized by its mean before averaging; time 0, call-onset. Inset: PSTH until 700 ms postcall; same  $y$ -range as main plot.

average 20% of their spatial selectivity (as indicated by the “20.0” coefficient in the regression equation above); (ii) the time-after-call explained 21% of the variance in the SSI;

(iii) the bat’s call-rate and velocity did *not* influence the SSI, so the reduction in the neurons’ spatial selectivity was a result of the passage of time after a call; (iv) significant changes in place-cell tuning were observable already within  $\sim 300$  ms after each call (Fig. 3B, right, “\*”), demonstrating that hippocampal place fields in big brown bats can change dynamically with rapid time constants of a few hundred milliseconds.

## Auditory Responses

To examine whether the post-sonar-call changes that we observed in place fields could be related to postcall changes in the *firing rate* of neurons on a fine time scale, we computed for each neuron a peristimulus time histogram (PSTH), showing spike rate triggered on echolocation calls. In other words, we used echolocation calls as triggering events (time 0) to examine auditory spiking responses in the bat hippocampus. Population-average PSTH showed *no* change in firing rate (Fig. 3F), all the way to 700 ms after the call (Fig. 3F, inset). This was supported by  $t$ -tests of precall vs. postcall firing rates in individual neurons: only two cells (2/32, 6%) exhibited any significant change in firing rate (in both cases, the firing rate slightly *decreased*). This lack of auditory responses is somewhat surprising, for the following reason. Several studies in rats have indicated that, typically, place cells do not exhibit auditory responses, unless the sound is made behaviorally important for the animal, such as in a conditioning paradigm (Shinba, 1999; Moita et al., 2003). One would expect that the bat’s own calls are behaviorally relevant, and therefore, the lack of sonar-evoked responses is somewhat surprising. We should point out that, to our knowledge, these data provide the first recording in any mammal of hippocampal neural activity in response to an animal’s own species-specific vocalizations. For comparative purposes, it would be of interest to determine if auditory evoked activity in rodent hippocampus occurs in response to the production of species-specific vocalizations.

Two conclusions can be drawn from Figure 3F: First, the absence of changes in firing-rate after a sonar call means that firing-rate changes alone cannot underlie the observed changes in place fields. Second, this demonstrates that even in the absence of changes in firing-rate (Fig. 3F, inset), spike-timing can affect the spatial information carried by spikes (Fig. 3B): this is an interesting example of temporal-based neural coding.

## Dynamics of Hippocampal Spatial Representation Linked to the Bat’s Exploratory Mode

Bats can explore space in one of two basic ways: either by moving through the environment (similar to rodents), or by scanning the environment from a fixed location using their distal sense of echolocation (similar to primates, which can use vision to explore space without locomoting). These two exploratory modes are characterized by two different types of action: In the first case the bat crawls linearly through space, whereas in the second case the bat scans the environment from a fixed location, using head movements to point the axis of its sonar

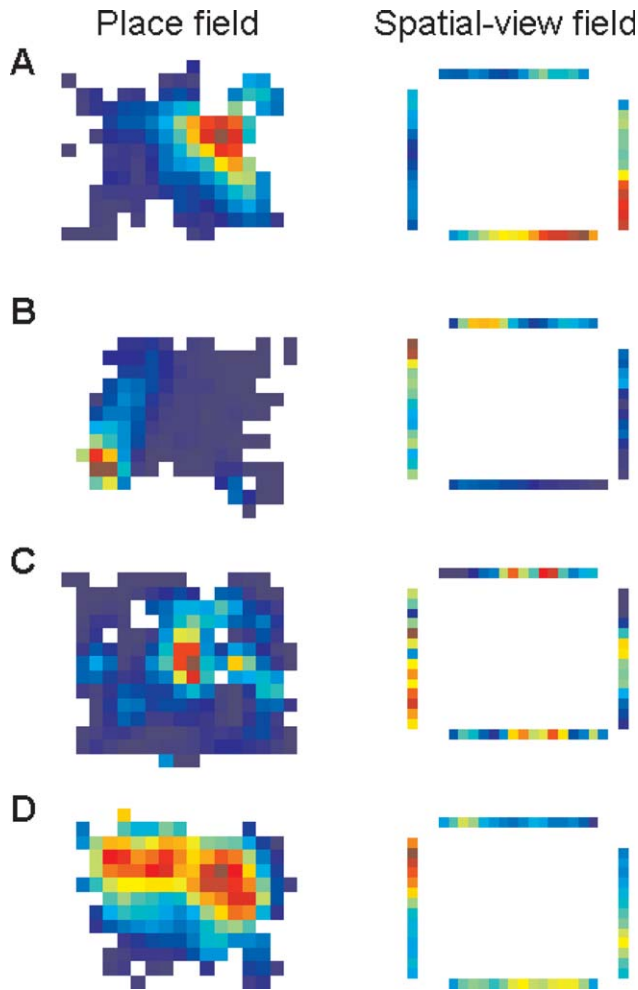


**FIGURE 4.** Spatial representation in the hippocampus of the big brown bat: examples of place fields (left) and spatial-view fields (right) from four neurons. (A) and (B) Two neurons that exhibited both a place field and a spatial-view field. (C) Example of a neuron exhibiting a place field in the center of the arena, but no spatial-view tuning. (D) A rare example of a neuron that exhibited a clear spatial-view field but only weak place tuning.

beam in different directions (Masters et al., 1985; Hartley and Suthers, 1989; Ghose and Moss, 2003). Therefore, we were interested in examining how the hippocampal spatial representation may be dynamically affected when the bat operates in these two behavioral modes.

Figure 4 shows examples of place fields (left) and “spatial view fields” (right) for several neurons recorded from bat hippocampal area CA1. The spatial view field (Rolls, 1999) quantifies the tendency of a neuron to discharge when the animal directed its head and sonar beam at a particular location on the arena wall (regardless of the animal’s location). The examples in Figure 4 show the variability across neurons. Many hippocampal cells exhibited both a place field and a spatial view field (e.g., Figs. 4A,B), while many others exhibited a place field without a spatial view field (e.g., Fig. 4C), and a couple of

neurons exhibited a narrow spatial view field but a very broad place field (e.g., Fig. 4D). We chose to plot the spatial view field because we wanted to explore some discrepancies in reports about spatial representation in *monkey* hippocampus. Specifically, some studies (Ono et al., 1993; Nishijo et al., 1997; Ludvig et al., 2004) have reported place-cells in primate hippocampus, whereas others (Rolls and O’Mara, 1995; Robertson et al., 1998; Georges-François et al., 1999) have reported finding spatial-view cells, but not place cells. As we show below, our results from the bat hippocampus may provide a surprising reconciliation of this apparent discrepancy.

To separate the two exploratory modes (locomotion vs. wall scanning) we plotted the bat’s linear velocity vs. angular velocity, and passed a diagonal line separating the data into two equal parts (Fig. 5A): A high-linear-velocity part, corresponding to locomotion behavior (Fig. 5A, red), and a high-angular-velocity part, corresponding to wall-scanning behavior (blue). This simplified delineation excludes overlap of the two behaviors and allows using 100% of the data (separated into two halves) and thus to reliably estimate the place fields and spatial view fields.

Figure 5B–D shows examples of three neurons, with each neuron analyzed separately according to the bat’s two behaviors (locomotion on left vs. wall scanning on right). These examples show that the wall-scanning behavior was characterized by more diffuse place fields and spatial view fields, and by lower maximal firing rates than the locomotion behavior. The same results were observed in population analyses (Fig. 6). Figure 6A shows the ratios of the peak firing rate between the locomotion/wall-scanning behaviors, for the place fields ( $x$ -axis) vs. spatial-view fields ( $y$ -axis). Peak firing rates, for both place-fields and spatial-view fields, were higher during locomotion than during wall-scanning behavior ( $t$ -test for the  $x$ -axis,  $x > 1$ :  $P < 0.01$ ;  $t$ -test for the  $y$ -axis,  $y > 1$ :  $P < 10^{-4}$ ; two-tailed tests). This corresponds to an increase in firing-rate with running speed, which is consistent with findings from rats that also reported increased peak firing-rates with increased running speed (McNaughton et al., 1983; Wiener et al., 1989).

Interestingly, the increase in peak firing-rate between the two behavioral modes in bats was more pronounced for the spatial-view fields than for the place fields, as indicated by most neurons falling above the  $x = y$  diagonal in Figure 6A ( $t$ -test:  $P < 0.01$ ). As we will argue below in the Discussion section, these results have some interesting implications for interpreting seemingly contradictory results on place-cells vs. spatial view cells in primate hippocampus (Ono et al., 1993; Rolls, 1999).

The coherence index of place fields and spatial view fields also changed between the two behaviors, in a manner that was consistent with the changes in peak firing rates. Figure 6B shows the difference of the coherence between the two behaviors (locomotion behavior - wall-scanning behavior), for the place fields ( $x$ -axis) vs. spatial-view fields ( $y$ -axis). The coherence of the spatial-view fields was higher during locomotion than during wall-scanning behavior ( $t$ -test for the  $y$ -axis,  $y > 0$ :  $P < 10^{-6}$ ), but no significant effect was observed for the place fields ( $t$ -test for  $x$ -axis:  $P = 0.74$ ). Again, most data-points in

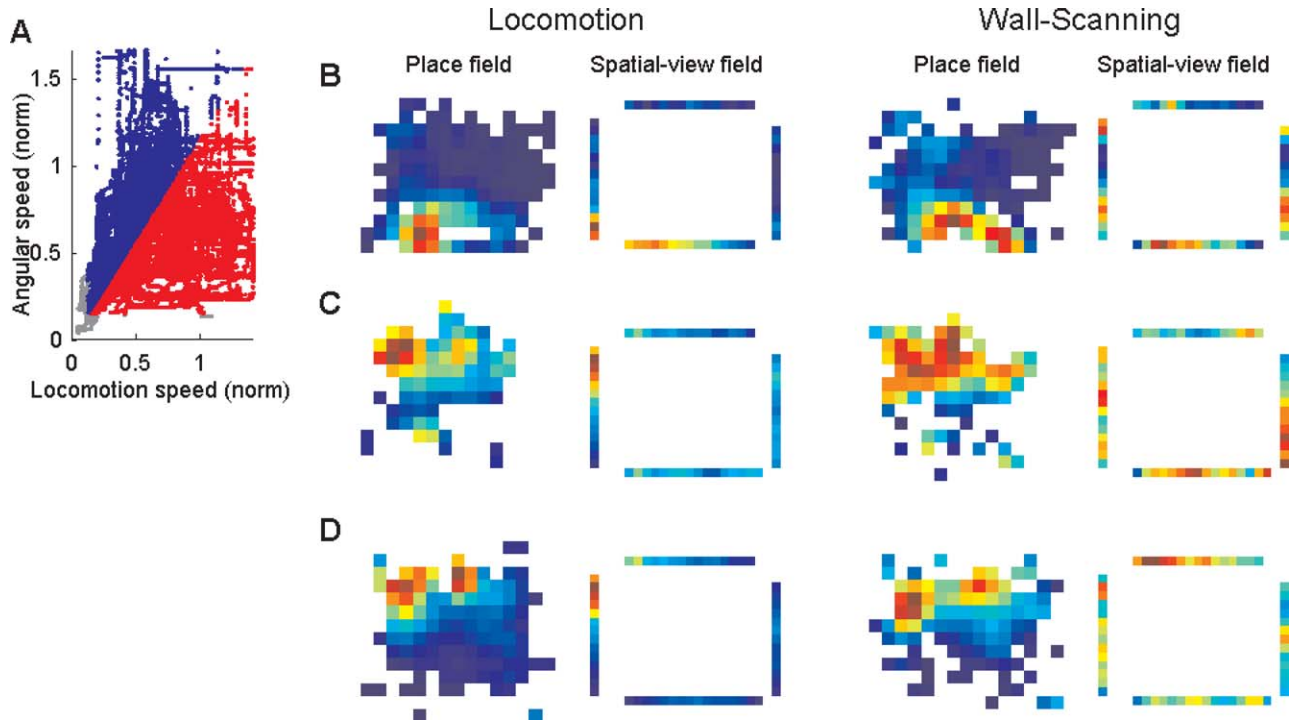


**FIGURE 5.** Dynamics of hippocampal spatial representation linked to the bat's exploratory mode: examples. (A) Example of the delineation of behavioral data from one session. The data were divided into epochs denoted "locomotion" or "wall scanning," based on whether the bat's linear velocity was more dominant ("locomotion," red dots) or whether angular motion was more dominant ("wall scanning," blue dots). The slope of the dividing diagonal line was chosen such that the total duration of locomo-

tion epochs was equal to that of wall-scanning epochs: i.e., the behavioral data were divided into two equal parts. (B) Place field and spatial-view field of a neuron, computed separately for the locomotion epochs (two panels on left) and for the wall-scanning epochs (two panels on right). Note that both the place-field and the spatial-view field become more diffuse during the wall-scanning epochs. (C and D) Additional examples of two neurons.

Figure 6B fell above the  $x = y$  diagonal ( $t$ -test:  $P < 10^{-5}$ ), indicating that the behavioral mode has a stronger effect on the spatial view field than on the place field.

Finally, we examined the time-course of transitions between the locomotion mode and wall scanning mode, by plotting the autocorrelation functions of the occurrence of the two modes (Fig. 6C). The autocorrelations in Figure 6C show time constants of  $\tau \sim 3$  sec; that is, the transitions between the two behavioral modes occurred typically every  $\sim 3$  sec. This means that the neural dynamics of place fields and spatial-view fields (Figs. 5 and 6) had a timescale of  $\sim 3$  sec.

## DISCUSSION

In sensory areas of the neocortex, such as primary visual cortex or primary auditory cortex, very rapid dynamics of tuning curves are revealed when using appropriate rapidly-presented stimuli as triggers (e.g., Ringach et al., 1997; deCharms et al., 1998; Elhilali et al., 2004). Here we studied rapid dynamics of place fields in bat hippocampus, using as triggers the bat's rapidly paced sonar calls (Figs. 2 and 3) and by dividing the data

according to two exploratory behavioral modes (Figs. 4–6). Our main finding was that individual hippocampal place fields can change much more rapidly than previously reported, with time-constants as short as  $\sim 300$  ms.

A few previous studies have reported relatively rapid time-constants for changes in hippocampal spatial representation. These studies differed from ours in several ways. Some studies have shown rapid dynamics based on the activity of populations of neurons (e.g., Redish et al., 2000; Johnson and Redish, 2007; Jackson and Redish, 2007)—without analyzing in detail the dynamics of *individual* neurons as we did here. Other studies looked at individual neurons, but the dynamics that they showed were on timescale of  $\sim 10$  sec (Frank et al., 2004; Wills et al., 2005)—at least one order of magnitude slower than the changes reported here. Finally, and most important, the dynamics shown in previous papers were linked to *internal* events—either shifts in spatial reference frames (Gothard et al., 1996; Redish et al., 2000; Johnson and Redish, 2007; Jackson and Redish, 2007) or changes within the theta cycle (e.g., Skaggs et al., 1996; Zugaro et al., 2005)—or they were not linked to any obvious events at all (Frank et al., 2004). In contrast, here we show dynamics of place-fields linked to *external*, sensory inputs.

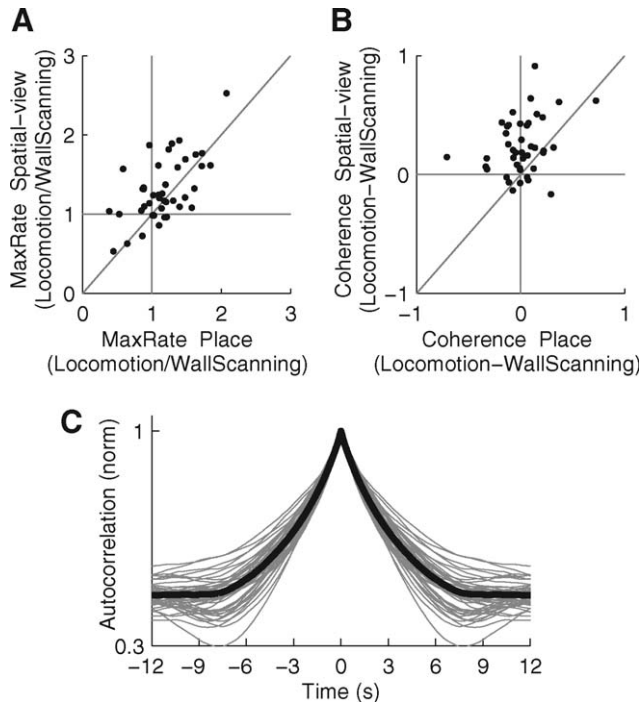


**FIGURE 6.** Dynamics of hippocampal spatial representation linked to the bat's exploratory mode: population analysis. (A) Scatter-plot showing on the *x*-axis the maximal firing-rate of the place field computed from locomotion epochs, divided by the maximal firing-rate of the place field computed from wall-scanning epochs; *y*-axis, same ratio for the maximal firing-rate of the spatial-view field. Dots, neurons (average values for the fields from the two behavioral sessions). Note that both the *x*-values and the *y*-values are  $>1$ , i.e., the firing-rate is higher during locomotion than during wall-scanning. (B) Similar plot to A, but using the coherence (Z-transformed) measure instead of the maximal firing-rate. For both panels (A) and (B) we took only cells for which data existed for both behavioral sessions, and for which the maximal firing-rate of the place field was  $>0.25$  Hz during both locomotion and wall-scanning behaviors ( $n = 42$  cells). (C) Autocorrelation of the transitions between the two behavioral modes ("locomotion" and "wall-scanning") for all the behavioral sessions (gray lines); black line, average autocorrelation.

### Place Fields Versus Spatial View Fields in the Hippocampus of Bats and Primates

The place-fields of bat hippocampal neurons were by far more pronounced than the spatial view fields of the same neurons. Thus, many neurons showed a place field without any spatial view field (e.g., Fig. 4C)—but we observed only 1 or 2 neurons where the opposite was true, i.e., the neuron had a very broad place-field but a narrow spatial view field (e.g., Fig. 4D). In other words, we found no evidence for pure "spatial view cells" in the hippocampus of the big brown bat.

An interesting aspect of these data was that the transitions between exploratory modes (locomotion vs. wall-scanning) exerted a stronger influence on spatial view fields than on place fields (Figs. 6A,B:  $y > x$ ). This effect of the animal's velocity is important, since it might explain the difference between Rolls's finding of spatial-view fields (Rolls and O'Mara, 1995;

Georges-François et al., 1999; Rolls, 1999) and Ono's finding of place-fields (Ono et al., 1993; Nishijo et al., 1997), both in monkey hippocampus. These monkey studies differed substantially in the animals' locomotion velocities: Rolls and colleagues reported that the monkeys in their experiments moved quite fast, up to 0.6 m/s (Georges-François et al., 1999), and they observed very dominant spatial view fields—corresponding to the enhanced dominance of spatial view fields in our data when the bats were moving fast (locomotion behavior). In contrast, Ono and colleagues reported that the monkeys in their studies were driving a small cab at extremely slow speeds, 5–10 cm/sec (Ono et al., 1993), and they observed clear place fields—corresponding to the enhanced dominance of place fields in our data when the bats were moving slowly (wall scanning behavior). Thus, our results in bats point to a possible reconciliation of seemingly contradictory reports on spatial-view fields vs. place fields in primate hippocampus.

### Rapid Modulation of Hippocampal Spatial Representation by the Bat's Sonar Calls

Our findings, as outlined in Figures 2 and 3, suggest the following picture (see schematic in Fig. 7): The sensory world of the big brown bat consists of a low acuity component, comprised of vision, olfaction, etc., interspersed with brief transient auditory inputs after each echolocation call, conveying high-resolution spatial information (Fig. 7A top, red). Each echolocation call sharpens the place cell's spatial selectivity, followed by a rapid decline in selectivity on a timescale of a few hundred milliseconds—creating sawtooth-like fluctuations in the neuron's spatial selectivity (Fig. 7A bottom, green). The decay of spatial-selectivity between sonar calls is consistent with studies in rats that showed reduced spatial-selectivity of place fields when sensory information is poor—e.g., in darkness (Markus et al., 1994), or when local olfactory cues are removed (Save et al., 2000). This reduction in spatial selectivity is likely caused by the use of "path integration" (Etienne and Jeffery, 2004; McNaughton et al., 2006), since path integration has been shown to be rapidly affected by drift, due to integration of errors, when no sensory stimuli are available for error correction (Etienne et al., 1998; Cheung et al., 2007).

Another intriguing question relates to the "rising-phase" of the sawtooth-like fluctuations (Fig. 7A bottom, *arrow*): Is there evidence that spatial tuning in the brain can sharpen on such ultra-fast time scales, of tens of milliseconds? In our hippocampal data it was impossible to measure place-field dynamics with such resolution (not enough spikes per time-bin). Notably, however, it was previously shown in the *auditory cortex* of the same bat species—the big brown bat—that auditory spatial tuning along the echo-delay (range) axis depends linearly on neural response latency. Response latencies of echo-delay tuned neurons (thought to encode the distance of sonar targets; Suga, 1989), spanned 8–40 ms, and those neurons with the longest response latencies showed the sharpest echo-delay tuning—suggesting that the bat's auditory cortex exhibits ultra fast sharpening of spatial encoding at the cell assembly level, following the

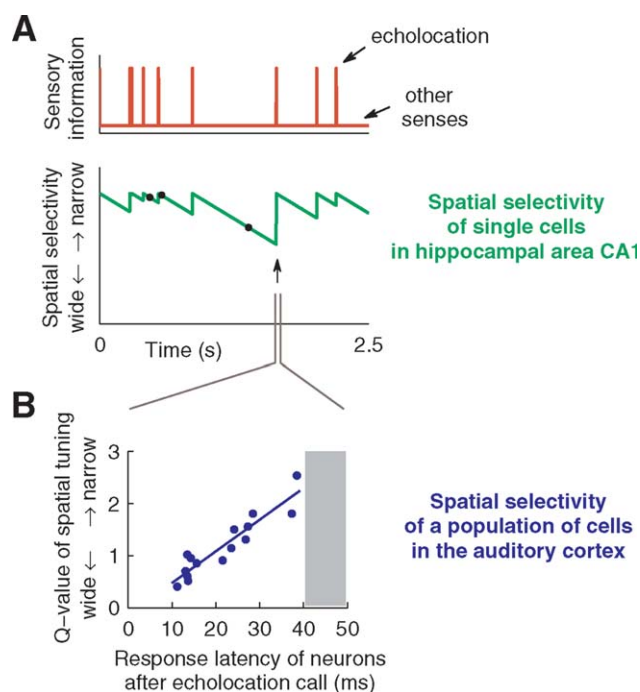


**FIGURE 7.** Schematic summarizing the rapid dynamics of bat hippocampal place-fields following an echolocation call (A) **Top:** Sensory inputs in the big brown bat consist of low-resolution information (visual, olfactory, etc.), interspersed with “stroboscopic” echolocation calls that bring a wealth of high-resolution sensory information within the echoes (Ulanovsky and Moss, 2008). The sequence of calls shown here was taken from Figure 2A. Our results suggest that each echolocation call “focuses” the spatial tuning of the place-field, making it narrower, and then place-fields rapidly broaden between the calls, within a  $\sim 1$ -s timescale—resulting in a sawtooth-like modulation (bottom, green trace). Black dots: spike times, illustrating that spikes occurring late after a call are carrying less spatial-information. (B) Hypothesis regarding the ‘rising-phase’ of the sawtooth (marked by *arrow* in panel A, bottom). Shown is the spatial-tuning width of a population of neurons from the bat’s auditory cortex (blue dots), plotted vs. the postcall response latency of the neurons (these experimental data were replotted from Dear et al., 1993). The spatial-tuning of this neuronal population becomes narrower, or more “focused,” within 40 ms after the sonar call—an ultra-fast time course (blue line, best linear fit). We hypothesize that this spatial-focusing may be transmitted from the auditory cortex to hippocampal CA1 neurons, via a series of projections, and account for the rising-phase of the sawtooth in panel A. Gray rectangle indicates that there are no neurons in this bat’s auditory cortex with discharge latency  $>40$  ms postcall (Dear et al., 1993)—so the hippocampus does not receive any auditory information during the long pauses between the sonar calls.

presentation of an echolocation call (Dear et al., 1993); these data are re-plotted in Figure 7B. We hypothesize that hippocampal place cells in area CA1 could inherit this ultra fast sharpening property from the auditory cortex, via the projections: auditory cortex  $\rightarrow$  auditory association cortex  $\rightarrow$  entorhinal cortex (EC)  $\rightarrow$  CA1.

An alternative interpretation of the rapid dynamics of place fields following each sonar call is that these dynamics are

caused by the motor act of producing the sonar vocalization. However, there does not seem to be an obvious mechanistic explanation for why the motor component of vocal production would cause a monotonic decrease in place-fields’ spatial selectivity (Fig. 3B). In contrast, the “sensory hypothesis” that we propose here—namely, that the decrease in spatial selectivity after each sonar call is caused by the lack of sonar sensory inputs (echoes) and thus the animal has to rely on path integration—seems more plausible.

There are several implications to our demonstration of place field modulation on the timescale of a few hundred milliseconds. First, the rapid dynamics of place fields (Figs. 2, 3, and 7) could contribute to out-of-field “noise” spikes that are observed in many place cells when place-fields are averaged over many minutes (Bostock et al., 1991; Wilson and McNaughton, 1993; Ulanovsky and Moss, 2007). To explore this issue we conducted simulations which demonstrated that in Gaussian-shaped place fields, adding an occasional expansion of the place field for only 5–10% of the time, led to a relatively high kurtosis of the place field, i.e., many outlier spikes, comparable to experimental results (data not shown). This suggests that at least one explanation for the existence of outlier spikes in place-cells may be that these spikes are not “noise” at all, but could reflect rapid neural dynamics.

Second, the dynamics of bat hippocampal place-fields are reminiscent of the dynamics of probabilistic robotic navigation algorithms (Thrun et al., 2005), where the “uncertainty ellipse” for the robot’s position is small when high-resolution, reliable sensor data are available—but the ellipse broadens when the robot has to rely on low-precision sensor data or on path-integration (see Thrun et al., 2005, their Fig. 10.3). This uncertainty ellipse behaves exactly analogously to the bat’s place fields (Figs. 2, 3, and 7).

Third, a previous study (Olypher et al., 2002) predicted the existence of a modulatory signal with a time scale of  $\sim 1$  sec in the hippocampus, as a means to explain the extreme variability (“overdispersion”) of rat place-cell firing during individual passes through the cell’s firing field (Fenton and Muller, 1998). The study by Jackson and Redish (2007) provided experimental evidence for such an ensemble modulatory signal in the hippocampus, which they interpreted as representing rapid switches between different reference frames in the hippocampus. Our results provide a complementary explanation for the phenomenon of overdispersion in place cells, namely, that place fields are modulated by the availability of sensory inputs (Figs. 2, 3, and 7). Additionally, we show that the firing of *individual* place cells (as opposed to network/ensemble dynamics) can indeed be modulated on the rapid time-scales predicted by Olypher et al. (2002).

## Predictions for Studies of Place Cells in Rodents

We hypothesize that the changes in place fields after each echolocation call occur, because during the “dark periods” between sonar calls the bat relies on path integration, and the information provided by path integration rapidly accumulates errors over time, and is then reset by the echo input from the

next sonar call. Analogously, we hypothesize that very rapid fluctuations of place-fields may occur also in the hippocampus of rats and mice. This hypothesis could be tested, for example, by having a rat or mouse forage in the dark in an open-field arena surrounded by visual cues, and repetitively flashing a strobe-light for 10 ms-ON/1-sec-OFF, while taking great care to eliminate local spatial cues such as self-deposited odor cues (Morris et al., 1982; Etienne et al., 1998; Save et al., 2000). If local cues are thoroughly eliminated (for example by continuously flushing any odors via constantly flowing water on the floor), then we predict that rat place fields would diffuse with the passage of time after the strobe-flash, similarly to our findings for the "stroboscopic" sonar system of bats. We expect that in such experiments the place cells in rat hippocampus will exhibit rapid changes on timescales of a few hundred milliseconds, similar to those reported here in echolocating bats.

More generally, we note that the long timescales typically observed in rat place-cell activity might be due to the relatively stable environments (long environmental timescales) in which rats are typically studied. We hypothesize that the time constants of the neural activity in the hippocampus reflect the time constants of behavior and of sensory information in the environment. Therefore one could unravel rich dynamics in rodent hippocampal place-fields by using richly dynamic environments.

## Acknowledgments

The authors thank M. Aytekin, K. Ghose, and S. David for comments on a previous version of the manuscript, A.D. Redish and K.D. Harris for helpful discussions, B. McNaughton, and G. Sutherland for technical advice, and E. Sanovich for histology.

## REFERENCES

- Bostock E, Muller RU, Kubie JL. 1991. Experience-dependent modifications of hippocampal place cell firing. *Hippocampus* 1: 193–205.
- Cheung A, Zhang S, Stricker C, Srinivasan MV. 2007. Animal navigation: The difficulty of moving in a straight line. *Biol Cybern* 97: 47–61.
- Dear SP, Simmons JA, Fritz J. 1993. A possible neuronal basis for representation of acoustic scenes in auditory cortex of the big brown bat. *Nature* 364:620–623.
- deCharms RC, Blake DT, Merzenich MM. 1998. Optimizing sound features for cortical neurons. *Science* 280:1439–1443.
- Eichenbaum H, Cohen NJ. 2001. *From Conditioning to Conscious Recollection: Memory Systems of the Brain*. Oxford: Oxford University Press.
- Elhilali M, Fritz JB, Klein DJ, Simon JZ, Shamma SA. 2004. Dynamics of precise spike timing in primary auditory cortex. *J Neurosci* 24:1159–1172.
- Etienne AS, Jeffery KJ. 2004. Path integration in mammals. *Hippocampus* 14:180–192.
- Etienne AS, Maurer R, Berlie J, Reverdin B, Rowe T, Georgakopoulos J, Seguinot V. 1998. Navigation through vector addition. *Nature* 396:161–164.
- Fenton AA, Muller RU. 1998. Place cell discharge is extremely variable during individual passes of the rat through the firing field. *Proc Natl Acad Sci USA* 95:3182–3187.
- Frank LM, Stanley GB, Brown EN. 2004. Hippocampal plasticity across multiple days of exposure to novel environments. *J Neurosci* 24:7681–7689.
- Georges-François P, Rolls ET, Robertson RG. 1999. Spatial view cells in the primate hippocampus: Allocentric view not head direction or eye position or place. *Cereb Cortex* 9:197–212.
- Ghose K, Moss CF. 2003. The sonar beam pattern of a flying bat as it tracks tethered insects. *J Acoust Soc Am* 114:1120–1131.
- Gothard KM, Skaggs WE, McNaughton BL. 1996. Dynamics of mismatch correction in the hippocampal ensemble code for space: Interaction between path integration and environmental cues. *J Neurosci* 16:8027–8040.
- Griffin DR. 1958. *Listening in the Dark*. New Haven, CT: Yale University Press.
- Hartley DJ, Suthers RA. 1989. The sound emission pattern of the echolocating bat, *Eptesicus fuscus*. *J Acoust Soc Am* 85:1348–1351.
- Jackson J, Redish AD. 2007. Network dynamics of hippocampal cell-assemblies resemble multiple spatial maps within single tasks. *Hippocampus* 17:1209–1229.
- Johnson A, Redish AD. 2007. Neural ensembles in CA3 transiently encode paths forward of the animal at a decision point. *J Neurosci* 27:12176–12189.
- Lee I, Rao G, Knierim JJ. 2004. A double dissociation between hippocampal subfields: Differential time course of CA3 and CA1 place cells for processing changed environments. *Neuron* 42:803–815.
- Leutgeb S, Leutgeb JK, Treves A, Moser M-B, Moser EI. 2004. Distinct ensemble codes in hippocampal areas CA3 and CA1. *Science* 305:1295–1298.
- Ludvig N, Tang HM, Gohil BC, Botero JM. 2004. Detecting location-specific neuronal firing rate increases in the hippocampus of freely-moving monkeys. *Brain Res* 1014:97–109.
- Markus EJ, Barnes CA, McNaughton BL, Gladden VL, Skaggs WE. 1994. Spatial information content and reliability of hippocampal CA1 neurons: Effects of visual input. *Hippocampus* 4:410–421.
- Masters WM, Moffat AJ, Simmons JA. 1985. Sonar tracking of horizontally moving targets by the big brown bat *Eptesicus fuscus*. *Science* 228:1331–1333.
- McNaughton BL, Barnes CA, O'Keefe J. 1983. The contributions of position, direction, and velocity to single unit activity in the hippocampus of freely-moving rats. *Exp Brain Res* 52:41–49.
- McNaughton BL, Battaglia FP, Jensen O, Moser EI, Moser M-B. 2006. Path integration and the neural basis of the 'cognitive map'. *Nat Rev Neurosci* 7:663–678.
- Mehta MR, Barnes CA, McNaughton BL. 1997. Experience-dependent, asymmetric expansion of hippocampal place fields. *Proc Natl Acad Sci USA* 94:8918–8921.
- Moita MA, Rosis S, Zhou Y, LeDoux JE, Blair HT. 2003. Hippocampal place cells acquire location-specific responses to the conditioned stimulus during auditory fear conditioning. *Neuron* 37:485–497.
- Morris RG, Garrud P, Rawlins JN, O'Keefe J. 1982. Place navigation impaired in rats with hippocampal lesions. *Nature* 297:681–683.
- Nishijo H, Ono T, Eifuku S, Tamura R. 1997. The relationship between monkey hippocampus place-related neural activity and action in space. *Neurosci Lett* 226:57–60.
- O'Keefe J, Nadel L. 1978. *The Hippocampus as a Cognitive Map*. Oxford: Oxford University Press.
- Olypher AV, Lánský P, Fenton AA. 2002. Properties of the extra-positional signal in hippocampal place cell discharge derived from the overdispersion in location-specific firing. *Neuroscience* 111:553–566.
- Ono T, Nakamura K, Nishijo H, Eifuku S. 1993. Monkey hippocampal neurons related to spatial and nonspatial functions. *J Neurophysiol* 70:1516–1529.

- Redish AD, Rosenzweig ES, Bohanick JD, McNaughton BL, Barnes CA. 2000. Dynamics of hippocampal ensemble activity realignment: Time versus space. *J Neurosci* 20:9298–9309.
- Ringach DL, Hawken MJ, Shapley R. 1997. Dynamics of orientation tuning in macaque primary visual cortex. *Nature* 387:281–284.
- Robertson RG, Rolls ET, Georges-François P. 1998. Spatial view cells in the primate hippocampus: Effects of removal of view details. *J Neurophysiol* 79:1145–1156.
- Rolls ET. 1999. Spatial view cells and the representation of place in the primate hippocampus. *Hippocampus* 9:467–480.
- Rolls ET, O'Mara SM. 1995. View-responsive neurons in the primate hippocampal complex. *Hippocampus* 5:409–424.
- Save E, Nerad L, Poucet B. 2000. Contribution of multiple sensory information to place field stability in hippocampal place cells. *Hippocampus* 10:64–76.
- Schnitzler H-U, Moss CF, Denzinger A. 2003. From spatial orientation to food acquisition in echolocating bats. *Trends Ecol Evolut* 18:386–394.
- Shinba T. 1999. Neuronal firing activity in the dorsal hippocampus during the auditory discrimination oddball task in awake rats: Relation to event-related potential generation. *Brain Res Cogn Brain Res* 8:241–250.
- Skaggs WE, McNaughton BL, Wilson MA, Barnes CA. 1996. Theta phase precession in hippocampal neuronal populations and the compression of temporal sequences. *Hippocampus* 6:149–172.
- Skaggs WE, McNaughton BL, Wilson MA, Markus EJ. 1993. An information-theoretic approach to deciphering the hippocampal code. In: Hanson SJ, Cowan JD, Giles CL, editors. *Advances in Neural Information Processing Systems* 5. San Mateo: Morgan Kaufman. pp 1030–1037.
- Squire LR. 1992. Memory and the hippocampus: A synthesis from findings with rats, monkeys, and humans. *Psychol Rev* 99:195–231.
- Suga N. 1989. Principles of auditory information-processing derived from neuroethology. *J Exp Biol* 146:277–286.
- Taube JS, Muller RU, Ranck JB Jr. 1990. Head-direction cells recorded from the postsubiculum in freely moving rats. I. Description and quantitative analysis. *J Neurosci* 10:420–435.
- Thrun S, Burgard W, Fox D. 2005. *Probabilistic Robotics*. Cambridge, MA: MIT Press.
- Ulanovsky N, Moss CF. 2007. Hippocampal cellular and network activity in freely moving echolocating bats. *Nat Neurosci* 10:224–233.
- Ulanovsky N, Moss CF. 2008. What the bat's voice tells the bat's brain. *Proc Natl Acad Sci USA* 105:8491–8498.
- Wiener SI, Paul CA, Eichenbaum H. 1989. Spatial and behavioral correlates of hippocampal neuronal activity. *J Neurosci* 9:2737–2763.
- Wills TJ, Lever C, Cacucci F, Burgess N, O'Keefe J. 2005. Attractor dynamics in the hippocampal representation of the local environment. *Science* 308:873–876.
- Wilson MA, McNaughton BL. 1993. Dynamics of the hippocampal ensemble code for space. *Science* 261:1055–1058.
- Zugaro MB, Monconduit L, Buzsáki G. 2005. Spike phase precession persists after transient intrahippocampal perturbation. *Nat Neurosci* 8:67–71.